



Phase Transformations

Prof. R. Chromik

Literature Research Project

Dynamic Recrystallization in Titanium Alloy TA-15: A Review

Daniel Bairos

Undergraduate

260331659

Submitted: 02/12/09

1. Introduction

TA-15 is a near-alpha titanium alloy often used for high-temperature aerospace applications.¹⁻⁵ Like many titanium alloys, it is sensitive to processing, making it fairly adaptable. However, TA-15 is difficult to deform under standard conditions.¹ Fabrication and forming must be done at elevated temperatures.¹ For this reason, it is important to understand and predict the thermo-mechanical response of this alloy.

It has been found that hot working of TA-15 often results in dynamic recrystallization of the material, where new equiaxed grains are formed simultaneously with deformation.¹⁻⁶ The effect is often a stronger and more ductile material, and in the case of TA-15, improved creep resistance.⁷ Understanding the hot deformation behaviour of this alloy is therefore central to controlling the resultant microstructure and properties. The objective of this review is therefore two-fold: i) to examine dynamic recrystallization and the parameters that affect its occurrence, evolution and morphology, ii) to observe dynamic recrystallization in alloy TA-15 and distinguish the effect of these parameters and how they can be useful in controlling microstructure and in turn, properties.

2. Review of Literature

2.1 Background on Near-alpha Titanium Alloys

Titanium alloy TA-15, also called BT20 or simply Ti-6Al-2Zr-1Mo-1V, is a Russian near-alpha alloy developed in 1964.⁴ Like many near-alpha alloys, it is often used for high-temperature applications – especially in the aerospace industry. Its high specific strength, thermal stability, corrosion resistance, inherent workability and weldability along with its good retention of mechanical properties at elevated temperatures, make it especially useful for aviation and aerospace engine components.^{1,4,8-10} For near-alpha alloys these often include: rotating components such as compressor discs and blades, as well as static high pressure compressor cases/brackets, spacer rings and exhaust mixers.⁷ Figure 1 shows a machined compressor disc made from TIMETAL 834⁹ a near-alpha alloy similar to TA-15 by way of its high-temperature stability.

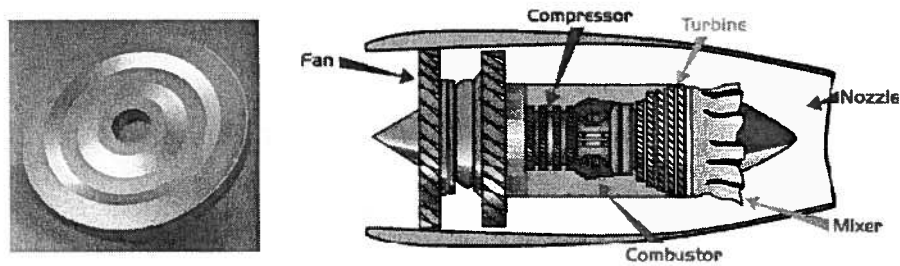


Figure 1. TIMETAL 834 (Ti-5.8Al-4Sn-3.5Zr-0.7Nb-0.5Mo-0.35Si-0.06C) compressor disc⁹ with schematic jet engine profile.¹¹

Near-alpha alloys often contain appreciable amounts of aluminum (approx. 2-7 wt%)¹⁰ that acts as an α -stabilizer in raising the α (HCP) \rightarrow β (BCC) transus temperature (883 °C for pure Ti), illustrated in Figure 2 (a).⁹ However, β -stabilizers like vanadium and molybdenum are frequently found in alloys of this type seeing as they improve processing characteristics and “permit greater manipulation of the microstructure of the material”.⁷ In addition, elements such as molybdenum and zirconium can increase passivity (i.e. corrosion resistance) and yield strength respectively.¹⁰ The result is a microstructure consisting primarily of α -grains with limited amounts of intragranular β -phase (Figure 2 (b)), hence, “nearly-alpha”.^{9,10} This is an important factor when considering the high-temperature properties of near-alpha alloys: the α -phase does not particularly respond to heat treatment, accounting for the retention of mechanical properties and good weldability.¹⁰ Operating temperatures of near-alpha alloys can go as high as 500 – 550 °C.^{7,9,10}

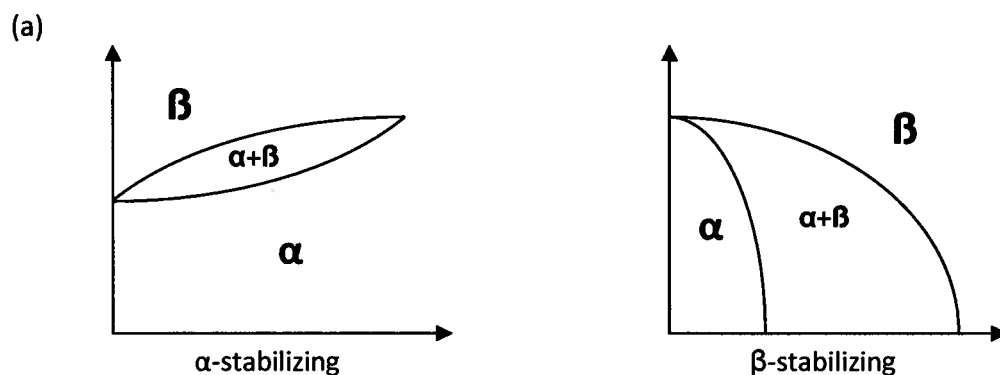


Figure 2. (a) α -stabilizing vs. β -stabilizing, adapted from Ref. 9.

(b)

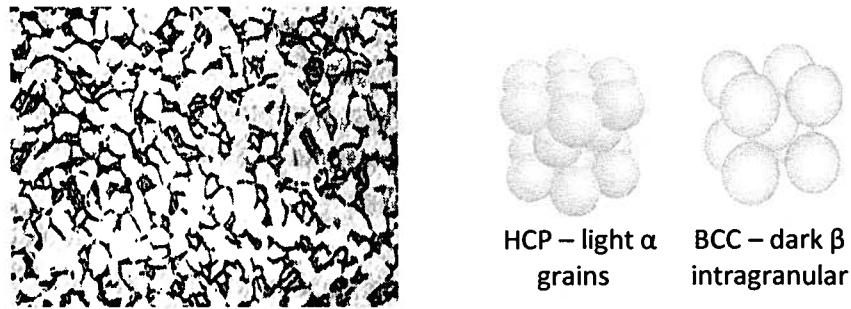


Figure 2. (b) Ti-6Al-4V micrograph¹⁰ ($\alpha+\beta$ alloy) showing light α (HCP)¹² grains and dark intragranular β (BCC)¹³.

Compared to the β -phase, α -Ti exhibits higher creep resistance and yield strength with reduced ductility.⁹ For this reason, forming and shaping of components are prone to fracture upon fabrication.¹⁴ “Recrystallization treatment” therefore makes for an important consideration when looking to manipulate the microstructure and final grain size of the material.¹⁰ On a whole, equiaxed α -grains – often a product of recrystallization – enhance the ductility and strength of the material along with creep and crack resistance,⁹ the latter leading to improved formability.^{10,15} Recrystallization inducing processes like thermal and thermo-mechanical treatments are therefore of great value when aiming for specific final properties that facilitate fabrication and improve performance.

Significant amounts of Al with minimal amounts of Mo and V give alloy TA-15 typical α -Ti characteristics. As a result, TA-15 is “very difficult to deform without heating”.¹ Hence, shaping of TA-15 is usually carried out at high temperatures by means of forging and forming processes.¹ For the above reasons, it is important to be able to predict the hot-deformation behaviour of this alloy and (as will be discussed in more detail below) it turns out that dynamic recrystallization is a frequent occurrence and is paramount in controlling grain size and morphology.³

2.2 Principles of Dynamic Recrystallization

Dynamic Recrystallization has been extensively studied. First indications of its occurrence were observed in the 1940’s when metals showed grain refinement after hot working.¹⁶ Since then, numerous hot deformation

experiments have been done in an attempt to properly understand, predict and model the nature of dynamic recrystallization, henceforth “DRX”.

The occurrence of DRX is most often recognized as abrupt onset of strain softening on a stress/strain curve for a material undergoing plastic deformation. Roberts and Bodén,¹⁷ who studied DRX behaviour in two austenitic stainless steels under axial compression between 1273 – 1573 K, illustrate the stress/strain behaviour of a typical DRX process shown in Figure 3.¹⁷ The general description of this schematic is that, after yielding, the material undergoes ordinary work-hardening until a peak value, at which point strain softening ensues – seen as a continual decline of stress with increasing strain – until finally a continuous or oscillatory steady-state is reached, depending on the temperature and strain rate, $\dot{\epsilon}$. Here, σ_c and ϵ_c represent critical stress/strain values at which point DRX begins.¹⁷

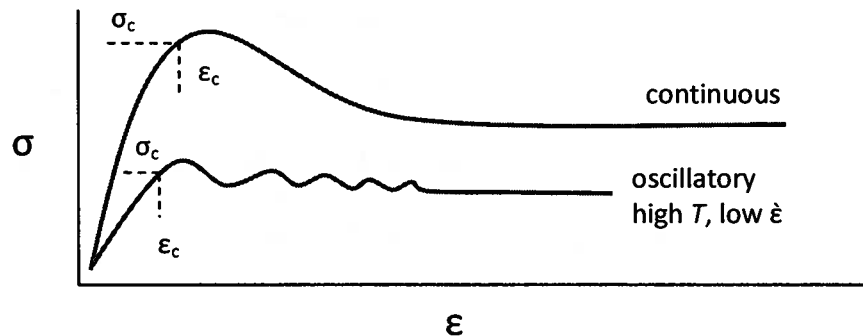


Figure 3. Schematic hot deformation σ/ϵ curves for materials undergoing DRX, adapted from Ref. 17.

Using Transmission Electron Microscopy and X-ray Diffraction to observe hot-rolled titanium alloy TA-15, Yong *et al.*⁵ showed that dislocation density increases with initial straining, then decreases to a constant range. This type of behaviour was also accepted by Sommitsch and Mitter,¹⁸ who performed hot compressive tests on a Nickel alloy in order to model DRX in low stacking fault energy metals. Here, dislocation density was the only parameter used to describe the onset of DRX. Other authors have stated the same; that dislocation density is a nucleation criterion for DRX.^{16,19-21} Thus, the critical stress/strain values σ_c and ϵ_c (usually slightly lower than the peak stress-strain values)^{19,22} correspond to a degree of deformation whereby dislocation density is at its

maximum and nucleation occurs thereafter. For this reason DRX is often found to occur in metals with low stacking fault energies where cross slip and climb systems are inefficient leading to a fast accumulation or “pileup” of dislocations at high strain points.^{1,3,23}

The driving force for DRX after the critical dislocation density has been reached is essentially the same for static recrystallization: nucleation will reduce stored energy difference in the strained lattice between dislocation-dislocation boundaries¹⁸ and nuclei can grow with a “continual loss in free energy”.¹⁷ Moreover, it is common to most authors that nucleation first occurs at pre-existing grain boundaries.^{16-22,24,25} In their model, Roberts *et al.*¹⁹ spoke of secondary nucleation sites being located at the original/new grain interface; a mechanism that would grow and finally consume the parent material. Sah *et al.*,²⁴ who conducted hot torsion experiments on nickel specimens, observed similar behaviour: nucleation occurred at original grain boundaries until all were exhausted (called “site saturation”) at which point “further grains were deposited on those already formed [i.e. interfacial boundaries] creating colonies which grew until the whole material was recrystallized”.²⁴ These types of nucleation mechanisms are supposedly common for initially fine grained material, however a coarser original grain size D_0 can bring about intragranular nucleation.^{18,19} With this in mind, it is worthwhile to note that the rate of DRX is increased by a decrease in D_0 .^{17,18,21,24}

To return to the oscillatory behaviour of the stress/strain curve, there is the impression that the reason for this occurrence is not completely understood. Sommitsch and Mitter explain that given ample time, recrystallized grains will impinge on each other enough such that the critical dislocation density is reached for a second time, allowing for DRX to occur over a second cycle.¹⁸ Hence, a cyclic stress/strain curve is often observed at low strain rates (allowing time for impingement), and high temperatures, thereby increasing dislocation mobility.^{17,18} Conversely, for higher strain rates and lower temperatures the start of DRX is seen as sizeable drop in flow stress (and/or true stress) in a “cascade” type recrystallization, followed by a steady-state flow. The steady-state is a result of an averaging of strains between the recrystallized and un-recrystallized material.²²

The Avrami kinetics of DRX has seldom been applied.²¹ By collecting and computationally reproducing literature data on 11 different steel specimens, Jonas *et al.*²¹ were able to generate Avrami plots for DRX based on the assumption that the fraction of material recrystallized is directly attributable to the net softening depicted on the stress/strain curves of hot deformed specimens.²¹ Figure 4 (a) shows a typical stress/strain curve adapted from Jonas *et al.*²¹ Here, σ_p and σ_{ss} represent peak and steady-state stress values respectively, together with $\Delta\sigma_s$ ("S" for softening): a parameter varying with instantaneous strain. The fractional softening X was then expressed as $X = \Delta\sigma_s / \sigma_p - \sigma_{ss}$.²¹ Using this equation Jonas *et al.*²¹ generated several $\ln(1/(1-X))$ vs. $\ln(t)$ plots which are presented in Figure 4 (b) as an example of DRX kinetics.

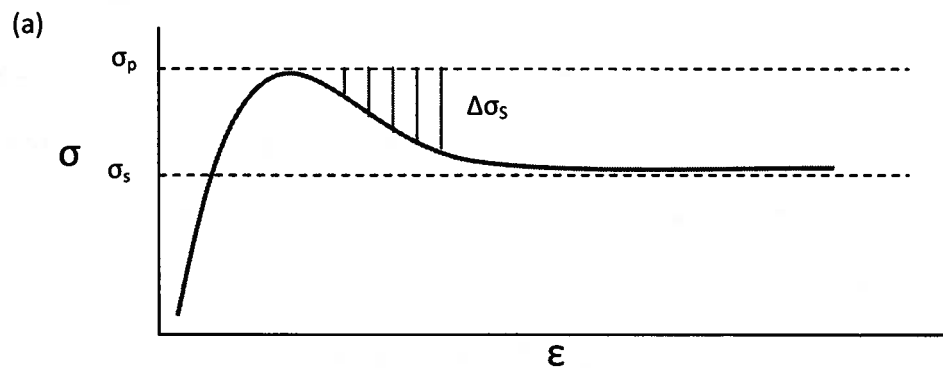


Figure 4. (a) Schematic hot deformation σ/ϵ curve, σ_p and σ_{ss} are peak and steady-state stress values respectively and $\Delta\sigma_s$, the net softening at an instantaneous strain. Adapted from Ref. 21.

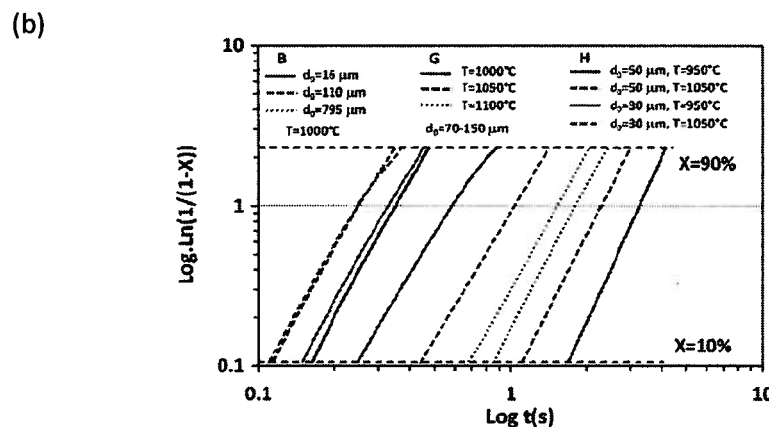


Figure 4. (b) $\ln(\ln(1/(1-X)))$ vs. $\ln(t)$ plots depicting a DRX 10-90% transformation on 11 different steels, taken from Ref. 21.

Looking at steels **G** and **H** in Figure 4 (b) it is apparent that the rate of DRX increases with temperature. Furthermore, looking at steels **B**, the relationship between rate and D_0 is as previously described: finer grains accelerate DRX.

The outcome of DRX is often an equiaxed microstructure, where grain size is dependant upon strain rate.^{17-19,22,24} Usually, the lower the strain rate the larger the final grain size since increased deformation time allows for additional grain growth i.e. a reduction in interfacial energy via grain boundary migration.^{23,24} Thus, initial grain size, deformation temperature and strain rate are important parameters for predicting how DRX will carry out and consequently, the resultant microstructure.

2.3 Dynamic Recrystallization in Alloy TA-15

Alloy TA-15 is not often used experimentally to demonstrate DRX. However, due to its low plasticity and high strength, forming of this alloy must be done at high temperatures.¹ For this reason, a good amount of literature exists dealing with the hot deformation behaviour in this alloy, and it has been found that DRX is to be expected.¹⁻⁶

All papers in this review conducted hot deformation experiments using a DSI Gleeble 1500 Simulator, APPENDIX A, Figure 1,²⁶ a thermo-mechanical testing apparatus. Using the Gleeble 1500, specimens are mounted and gripped in a vacuum atmosphere and deformed using a standard air piston. Through electrical-resistance heating, high-temperature results (like stress/strain curves) are generated and plotted on a computer screen.²⁶ Prior to testing, samples were held at the deformation temperature for approximately 1 to 10 minutes.¹⁻⁶ Microstructural analysis and Transmission Electron Microscopy were the principle methods for observing microstructural evolution.

Figure 5 shows the initial, pre-hot-worked, TA-15 microstructures of 3 specimens taken from Refs. 2, 4, 8. Light regions are α -lamellae while dark regions are intragranular β -phase found in small quantities.^{4,15} The common consensus is that the $\alpha + \beta \rightarrow \beta$ transition temperature for TA-15 is in the range of 970 – 980 °C.^{1,2,4} This became an important factor in describing the microstructures of specimens deformed near this range and

will be discussed in more detail below. In addition, Yong *et al.*² described the initial TA-15 microstructure as having “little dislocations” based on their TEM micrograph, Figure 5 (d), showing the α/β phase boundary.²

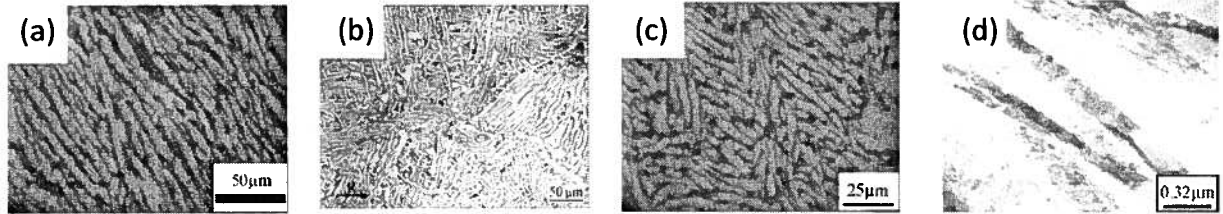


Figure 5. Initial pre-hot-worked TA-15 microstructures. (a) from Ref. 2 (b) Ref.8 (c) Ref. 4 (d) Ref. 2

All hot compressive experiments done on TA-15 showed the same trend: stress decreases with increasing deformation temperature and decreasing strain rate.^{1,2,4-6} More importantly, the stress/strain curves illustrate peak values followed by strain softening – a typical indication of DRX. Xu *et al.*,⁶ who performed axial hot compression tests at different temperatures/strain rates on TA-15, stated that “the main softening mechanism may be DRX”.¹ Their results are shown in Figure 6.¹

It can be seen from Figure 6 that at temperatures ranging from 650 to 850 °C softening is more pronounced, whereas at low temperatures of 550 to 600 °C a significant drop in stress is not apparent nor is it at high temperatures, 900 to 1000 °C, where stress remains relatively constant.¹ In order to account for the observed behaviour, Xu *et al.*¹ put emphasis on the distinction between deformation mechanisms; essentially plastic deformation, DRX and a phase transformation. At 550 and 600 °C, it can be seen from Figure 6 that strain rates of 0.1 and 0.01 s⁻¹ show the same stress/strain response i.e. work hardening. According to Xu *et al.*,¹ the same trend would have been observed at $\dot{\epsilon} = 1 \text{ s}^{-1}$ had it not been for the low thermal conductivity of Ti (14.99 W/mK for Ti (Ref. 9) compared to 80.4 W/mK for Fe (Ref. 27)) causing local temperature increases in the material as a result of a faster rate of shearing deformation. The authors showed that, at low temperatures, this increase could be significantly large – in the order of 20% at 550 °C.¹ This “deformation heat” would possibly increase the material temperature sufficiently for DRX to occur, causing a slight drop in the stress/strain curve.

Figure 7 (a), (b), (c) shows the optical micrographs of specimens tested at 650 °C for $\dot{\epsilon} = 1, 0.1, 0.01 \text{ s}^{-1}$ ($\epsilon = 65\%$) respectively.¹ Observing these microstructures, evidence of plastic deformation can be seen as typical elongated or pancaked grains and therefore the micrographs are in agreement with the above description i.e. that work hardening is the primary mechanism of deformation in the material at low temperatures.¹ The authors note, however, that DRX has occurred to a certain extent, but is not the primary deformation mechanism. Note that while Xu *et al.*¹ did not describe nor supply a micrograph of the original TA-15 microstructure, it is assumed to be α -lamellar. Micrographs are also assumed to be of air cooled specimens, taken parallel to the compression axis, based on other reports.^{2,4,6}

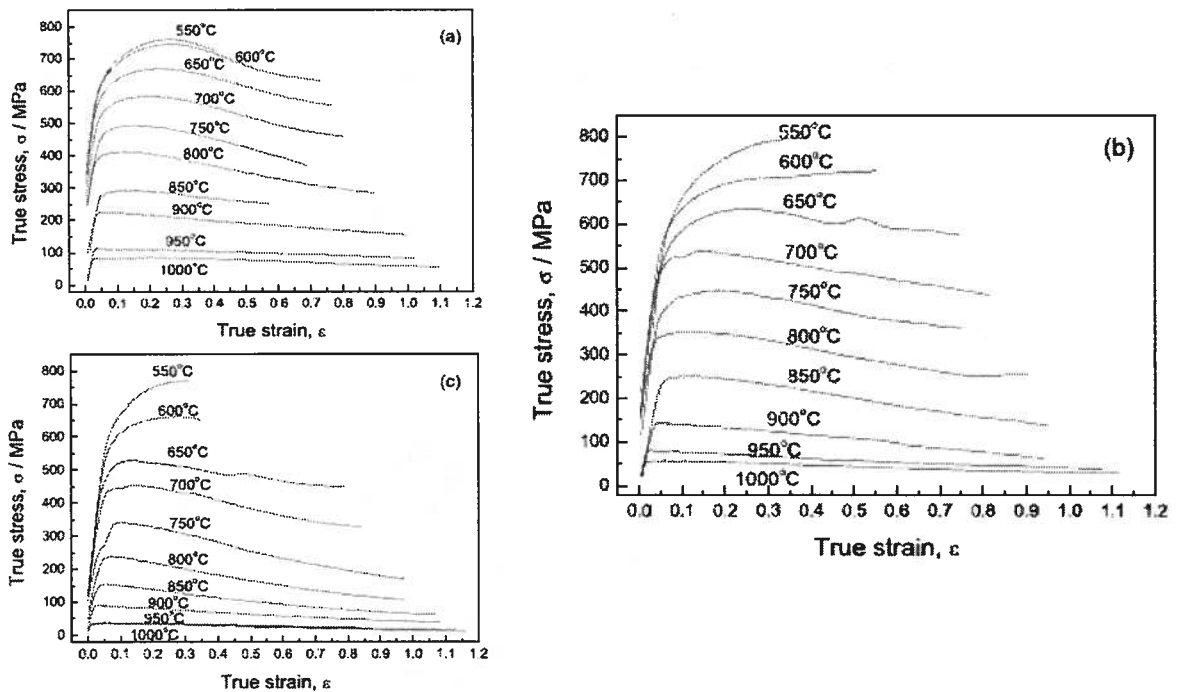


Figure 6. True stress vs. true strain for hot deformation of TA-15 taken from Ref. 1. (a) 1 s^{-1} , (b) 0.1 s^{-1} , (c) 0.01 s^{-1}

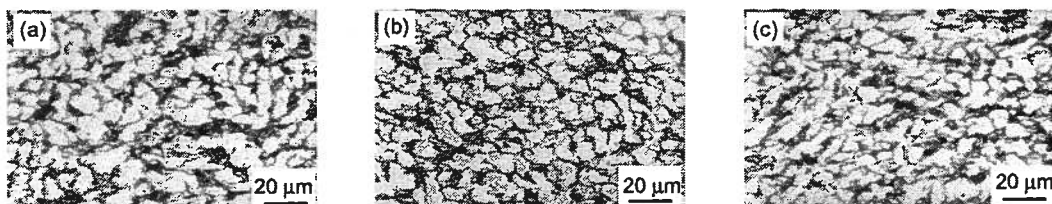


Figure 7. TA-15 optical micrographs of specimens hot compressed at 650 °C at different strain rates ($\epsilon = 65\%$), taken from Ref. 1. (a) $\dot{\epsilon} = 1 \text{ s}^{-1}$, (b) $\dot{\epsilon} = 0.1 \text{ s}^{-1}$, (c) $\dot{\epsilon} = 0.01 \text{ s}^{-1}$

Xu *et al.*¹ only included constant strain rate micrographs for $\dot{\epsilon} = 1 \text{ s}^{-1}$. Figure 8 (a) and (b) shows these micrographs for 800 and 900 °C respectively. Looking at these micrographs the authors point out that DRX has occurred based on the apparent equiaxed grains inherent in the microstructure.¹ The more prominent dark regions found at 900 °C are presumably β -Ti – a result of several localized $\alpha + \beta \rightarrow \beta$ transformations occurring within the material due to the deformation heating.¹ These conclusions are also in correspondence with the stress/strain response at 800 and 900 °C, Figure 6 (a), where softening at 800 °C is more pronounced than at 900 °C. This is due to fact that β -Ti has a BCC crystal structure which has higher stacking fault energies, consequently impeding DRX.¹ Similarly, the primary deformation mechanism at high temperatures ($T > 900 \text{ °C}$) was concluded to be a phase transformation.¹ To elaborate on this point, at 1000 °C all microstructures exhibited a needle-shaped martensitic appearance due to a complete $\alpha + \beta \rightarrow \beta$ phase transformation (Figure 8 (c) (d)).¹

Further support for the occurrence of DRX can be seen by looking at Figure 8 (e), $T = 800 \text{ °C}$ and $\dot{\epsilon} = 0.01 \text{ s}^{-1}$. Comparing with the specimen strained at the same temperature but higher strain rate i.e. Figure 8 (a), the specimen tested at a lower strain rate displayed an apparent increase in grain size, a result of greater deformation time allowing for grain growth.^{18,22}

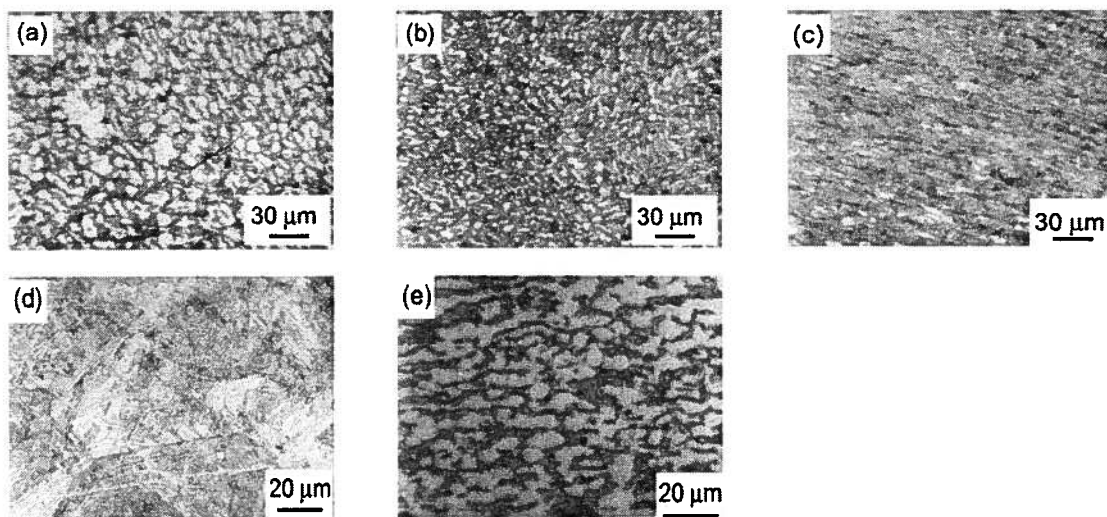


Figure 8. Hot compressed TA-15 optical micrographs ($\epsilon = 65\%$), taken from Ref. 1. (a) $T = 800 \text{ °C}$, $\dot{\epsilon} = 1 \text{ s}^{-1}$ (b) $T = 900 \text{ °C}$, $\dot{\epsilon} = 1 \text{ s}^{-1}$ (c) $T = 1000 \text{ °C}$, $\dot{\epsilon} = 1 \text{ s}^{-1}$ (d) $T = 1000 \text{ °C}$, $\dot{\epsilon} = 0.01 \text{ s}^{-1}$ (e) $T = 800 \text{ °C}$, $\dot{\epsilon} = 0.01 \text{ s}^{-1}$

It turns out that, along with DRX, the formation of acicular β -Ti is a prominent result of hot working. Commonly called a Widmanstatten microstructure,^{4,10} such is frequently observed in Ti alloys that are slowly cooled from temperatures near or above the β transus.¹⁰ Like Xu *et al.*,¹ Wang *et al.*,⁴ after air-cooling hot compressed specimens of TA-15, observed the same gradual increase in dark β regions with respect to increasing deformation temperature. Micrographs of deformed specimens tested at constant strain rate ($\dot{\epsilon} = 0.01 \text{ s}^{-1}$) are presented in Figure 9.⁴ Here, β regions are found forming at α boundaries with amounts increasing with respect to temperature until a final needle-like Widmansatten microstructure at 1000 °C (Figure 9 (c)).⁴ Figure 10 illustrates this trend as a plot of α -volume fraction as a function of deformation temperature, reproduced from the results of Wang *et al.*⁴. Note that β begins to form even below the β transus temperature, possibly due to deformation heat explained by Xu *et al.*¹ Unlike most literature,^{1-2,6} Wang *et al.*⁴ did not find the DRX to be a principle mechanism during hot working. In other words, equiaxed grains were not observed.

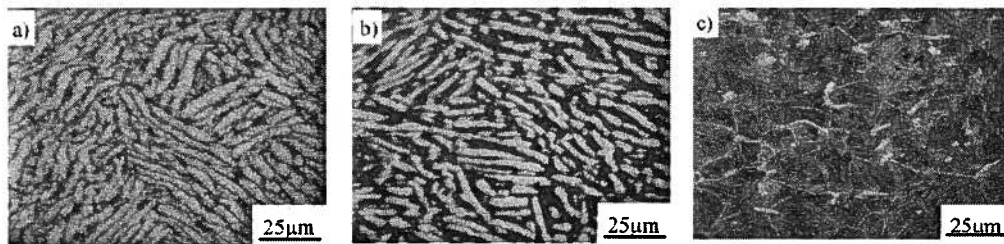


Figure 9. TA-15 optical micrographs compressed at $\dot{\epsilon} = 0.01 \text{ s}^{-1}$ (ϵ unspecified), taken from Ref. 4. (a) T = 800 °C (b) T = 900 °C (c) T = 1000 °C

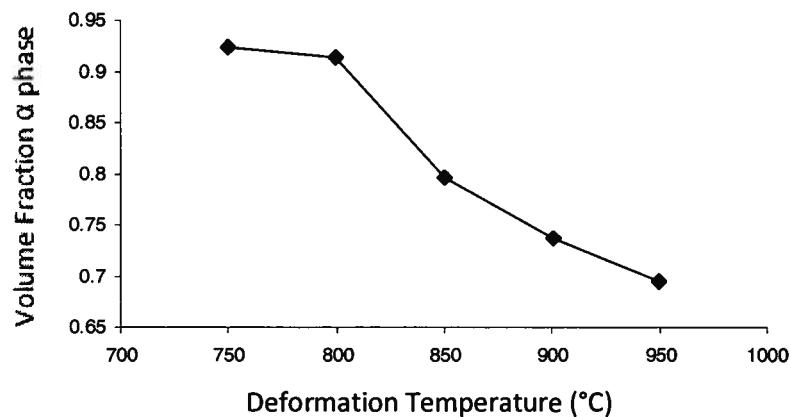


Figure 10. Effect of deformation temperature on volume fraction of primary α -phase, re-plotted from Ref. 4.

In an attempt to examine to the kinetics of DRX in TA-15, the method derived by Jonas *et al.*,²¹ whereby the fraction recrystallized is defined by the equation $X = \Delta\sigma_s / \sigma_p - \sigma_{ss}$, was applied to the hot compression result of Yong *et al.*² (APPENDIX B, Figure 1 (a) (b)). Using a program called Data Extractor, points along the stress/strain curve were tabulated for 800 °C and $\dot{\epsilon} = 0.01 \text{ s}^{-1}$. Results are shown in APPENDIX B, Table 1. Subsequently, X and $\ln(1/(1-X))$ were plotted as a function of $\ln(t)$ and did in fact show respective sigmoidal and straight line relationships – characteristic of recrystallization. Plots can be found in APPENDIX B, Figure 2 (a) (b). It is worthwhile to note that, through microstructural analysis, Yong *et al.*² also concluded DRX to be a defining mechanism of TA-15 under thermo-mechanical forming; the authors conclude that an apparent decrease in grain size together with a common “equiaxial tendency” “can be attributed to recrystallization”.² The micrographs included were small and unclear and therefore were not included in this review.

Finally, a model for DRX in TA-15 was proposed by He,³ who used the Cellular Automata Model to simulate DRX based primarily on the assumption that DRX will initiate after a critical dislocation density in the material is reached.³ Other considerations made by He³ are of great value when it comes to understanding DRX – re-stated:

- i. The initial input microstructure is entirely α -lamellar.
- ii. Once critical dislocation density is reached, the DRX process will begin.
- iii. The dislocation density of a new grain is zero, and will increase with further deformation.
- iv. Nucleation occurs at both primary and interface grain boundaries.

Without going into details of the sub-model used for dislocation mobility and accumulation, He³ was able to generate stress/strain curves that are consistent with literature.^{1,2,4,6} Model results are presented in Figure 11³ and are compared with actual optical micrographs of which no mention of experimental procedure was included. Note that images are snapshots of the ongoing deformation. Looking at Figure 11 the above considerations are evident and, more importantly, the final microstructure is equiaxed in both the generated and actual images.³ Furthermore, He³ concluded that “with the increase of strain rate, the mean diameter of

DRX-grains decreases” – illustrated in Figure 12. This is in accordance with the results of Xu *et al.*¹ and implies that grain growth is only favourable when ample time is allowed. Thus, a coarser grain size can be achieved by decreasing the deformation rate.

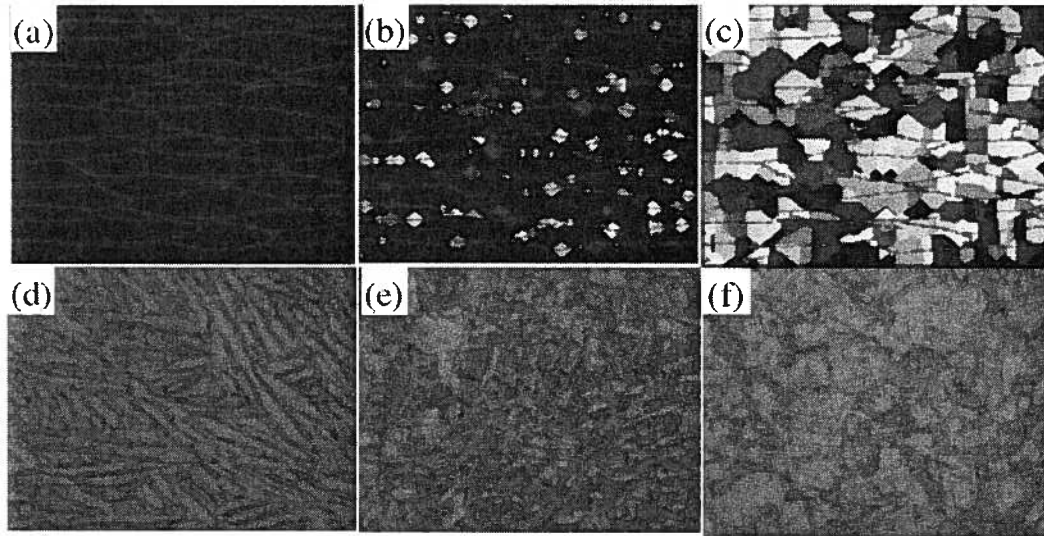


Figure 11. Simulated vs. experimental results of microstructural evolution of hot compressed TA-15 at 800 °C and a strain rate of $\dot{\epsilon} = 0.001 \text{ s}^{-1}$, taken from Ref. 3. (a),(d) $\epsilon = 0 \%$; (b),(e) $\epsilon = 60 \%$; (c),(f) $\epsilon = 70 \%$

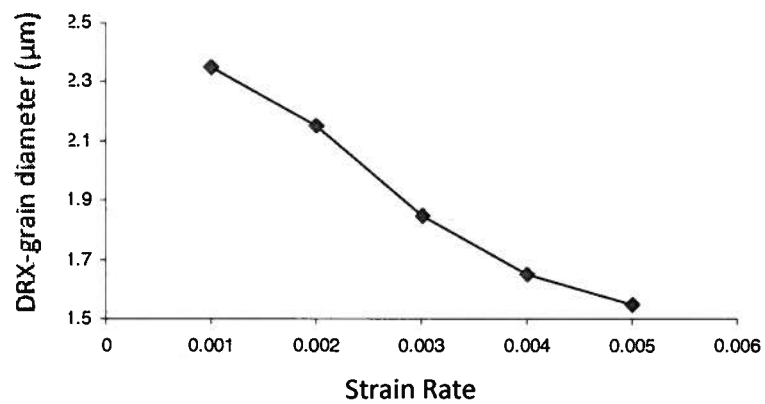


Figure 12. Effect of strain rate on DRX grain size, re-plotted from Ref. 3.

2.4 Discussion

The above account described the relative parameters affecting DRX, namely, deformation temperature and strain rate. The third parameter, D_0 , was not considered in the literature, perhaps because variation of D_0 , above all, affects the rate of DRX. Certainly an important factor for processing, literature on the topic would be valuable for a complete assessment of the thermo-mechanical response of TA-15. While no mention of the effect of DRX in TA-15 with respect to mechanical properties was discussed in the above mentioned papers, from sections 2.1 and 2.2, insight can be added.

For one, it is likely that DRX would be favourable when forming TA-15 as equiaxed grains improve strength and ductility.^{9,10} However, while acicular microstructures often exhibit superior fatigue performance and higher fracture toughness compared to an equiaxed α -Ti matrix, a fully transformed β -Ti microstructure would certainly diminish the thermal stability of the alloy.^{9,10} The temperature dependent relative amounts of α and β -phase are therefore an important consideration for the application of the material. The trend observed by He³, namely the inverse relation between strain rate and DRX-grain size, is also important in that the final grain size of the material can be controlled. For example, coarser grains would be desirable for centrifugally loaded rotating aeroengine components as they improve creep resistance.¹⁰ On a final note, based on the results from Refs. 1 and 4, it is likely possible to avoid DRX at temperatures between 550 – 600 °C since work hardening was shown to be the primary deformation mechanism in this range, with no mention of cracking or tearing.

3. Summary

Titanium alloy TA-15 is a near-alpha alloy, readily used for high-temperature aerospace applications. Like most near-alpha alloys, its low plasticity makes it hard to form at room temperature. For this reason the hot deformation behaviour has been reviewed. It was found from literature that hot deformation often led to an equiaxed microstructure with more prominent β -phase amounts. This, along with the experimental stress/strain relationship, was a primary indication that recrystallization was occurring at the same time as deformation.

Research on this type of behaviour, namely dynamic recrystallization, showed how deformation temperature, strain rate and initial grain size affect the progression of DRX and the final microstructure of the material. The same trends were observed in alloy TA-15, namely that grain size increases with decreasing strain rate and that the resultant microstructure is equiaxed. Coarse grains and equiaxed microstructures were seen as positive products of processing since ductility, strength and creep resistance are increased. Alongside these observations, an $\alpha + \beta \rightarrow \beta$ (acicular) phase transformation was found to occur at higher deformation temperatures near the β transus. From the literature on Titanium,^{7,9,10} it was concluded that the formation of a β -Ti acicular microstructure is undesirable since the alloy would lose its high temperature stability and therefore lower its operating temperature.

4. References

1. Xu Wen-chen et al., J. Mater. Sci. Technol. **21**, 807 (2005).
2. Liu Yong et al., Mater. Sci. Eng. A **490**, 113 (2008).
3. Dong He, Int. J. Modern Phys. **23**, 934 (2009).
4. Y. Wang et al., J. Mater. Sci. Technol. **21**, 1466 (2005).
5. Lui Yong et al., J. Wuhan Uni. Technol. Mat. Sci. Ed. **24**, 202 (2009).
6. Xu Wen-chen et al., Trans. Nonferrous Met. Soc. **16**, 2066 (2006).
7. R. R. Boyer, Mater. Sci. Eng. **A213**, 103 (1996).
8. Fan Rong-hui et al., Trans. Nonferrous Met. Soc. **17**, 482 (2007).
9. C. Leyens and M. Peters, Titanium and titanium alloys: fundamentals and applications, (Wiley-VCG, Weinheim, 2003) p. 1-36, 289-304.
10. Matthew J. Donachie, Jr., Titanium a Technical Guide, 1st ed. (ASM International, Ohio, 1988) p.13-36, 50-62
11. About.com, Inventors, "Parts of a Jet Engine", November 17, 2009,
<http://inventors.about.com/library/inventors/blhowajetengineparts.htm>.

12. Department of Metals and Materials Science, University of Cambridge, "Metallurgy of Titanium and its Alloys", November 17, 2009, <http://www.msm.cam.ac.uk/phasetrans/2003/titanium.movies/titanium.html>.
13. Tripod.com, Erik's Chemistry, "Chemistry Images" November 17, 2009, <http://members.tripod.com/~EppE/images.htm>.
14. Wikipedia the Free Encyclopedia, "Forging", November 19, 2009, <http://en.wikipedia.org/wiki/Forging>.
15. L. Germain et al., *Acta Mater.* **56**, 4298 (2008).
16. H.J. McQueen, *Mater. Sci. Eng. A* **387-389**, 2003 (2004).
17. W. Roberts, H. Boden, and B. Ahlblom, *Metal Sci.* **13**, 195 (1979).
18. C. Sommitsch, W. Mitter, *Acta Mater.* **54**, 357 (2006).
19. W. Roberts and B. Ahlblom, *Acta Metall.* **26**, 801 (1978).
20. Siamak Serajzadeh, *Modelling Simul. Mater. Sci. Eng.* **12**, 1185 (2004).
21. John J. Jonas et al., *Acta Mater.* **57**, 2748 (2009).
22. T. Sakai and J. J. Jonas, *Acta Metall.* **32**, 189 (1984).
23. Darcy A. Hughes and Niels Hansen, *ASM Handbook Volume 9: Metallography and Microstructures, Plastic Deformation Structures*, (Materials Information Society, Ohio, 2004) p. 192-214.
24. J. P. Sah, G. J. Richardson, and C. M. Sellars, *Metal Science.* **8**, 325 (1974).
25. Frank Montheillet and Jean-Phillippe Thomas, *NATO Sci. Series* **146**, 357 (2004).
26. Center for the Accelerate Maturation of Materials, Ohio State, "The Gleeble..." November 16, 2009, <http://members.tripod.com/~EppE/images.htm>.
27. Wikipedia the Free Encyclopedia, "Iron", November 19, 2009, <http://en.wikipedia.org/wiki/Iron>.

APPENDIX A – DSI Gleeble 1500 Simulator

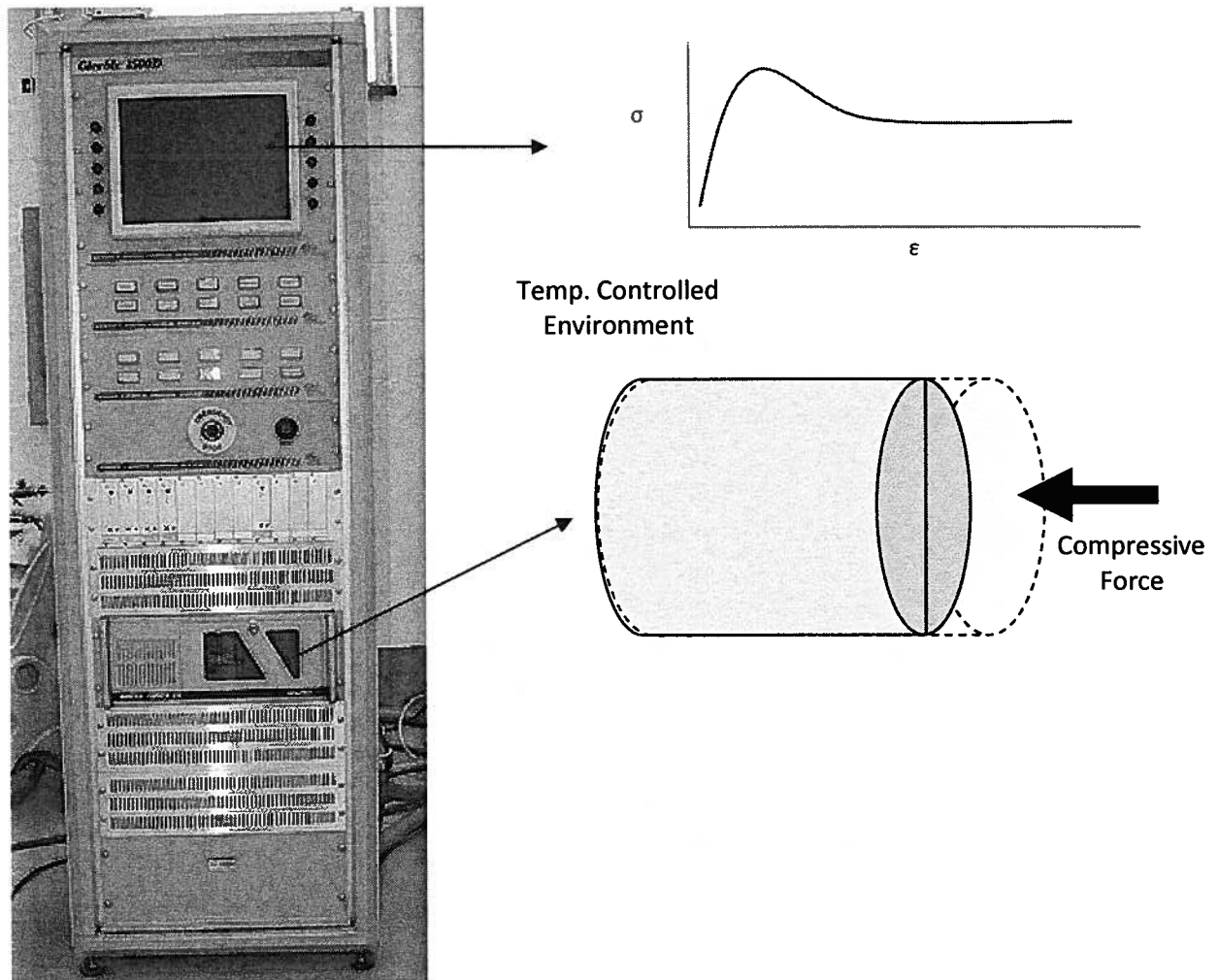


Figure 1. DSI Gleeble 1500 Simulator,²⁶ a thermo-mechanical testing apparatus.

APPENDIX B – Method of Jonas *et al.*²¹ applied to results of Yong *et al.*²

Table 1. Fraction Recrystallized and $\Delta\sigma_s$ graphically attained from Yong *et al.*²

$\Delta\sigma_s$	X	$\ln(t)$	$\ln(\ln(1/1-X))$
12.102	0.096	2.220	-2.293
20.723	0.164	2.582	-1.717
31.076	0.247	2.883	-1.262
39.703	0.315	3.080	-0.972
48.319	0.383	3.254	-0.726
55.191	0.438	3.389	-0.551
65.557	0.520	3.520	-0.308
72.376	0.574	3.626	-0.157
77.375	0.614	3.734	-0.049
83.294	0.661	3.823	0.079
87.413	0.694	3.910	0.168
94.121	0.747	4.008	0.318
99.283	0.788	4.076	0.439
103.608	0.822	4.141	0.547
107.038	0.850	4.201	0.639
110.474	0.877	4.255	0.739
116.589	0.925	4.314	0.953
119.113	0.945	4.366	1.067
119.834	0.951	4.415	1.104
119.665	0.950	4.459	1.095
120.358	0.955	4.511	1.133

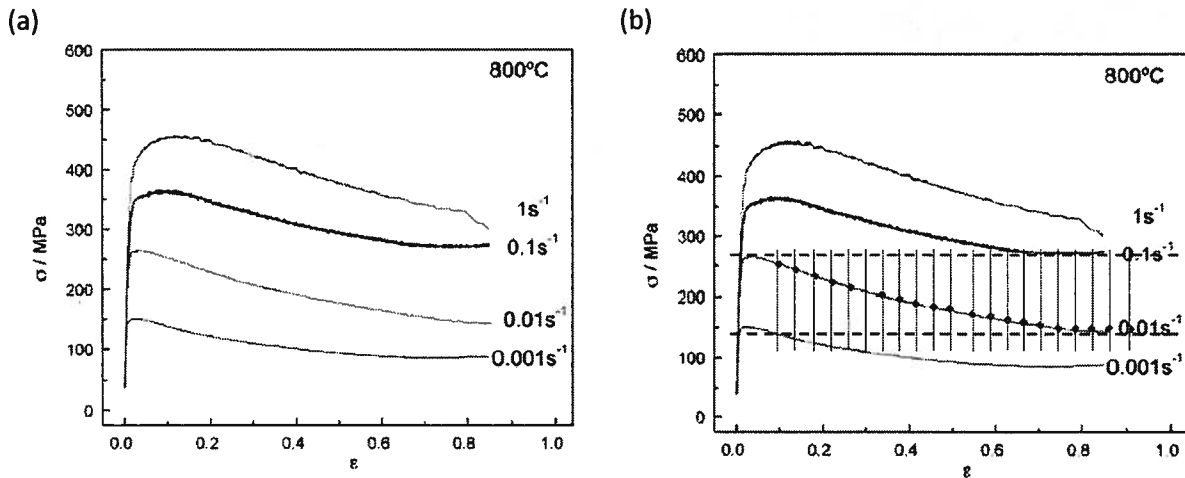


Figure 1. (a) stress vs. strain for compression tests on alloy TA-15 at 800 °C.² (b) 21-point method of analysis based on Jonas *et al.*

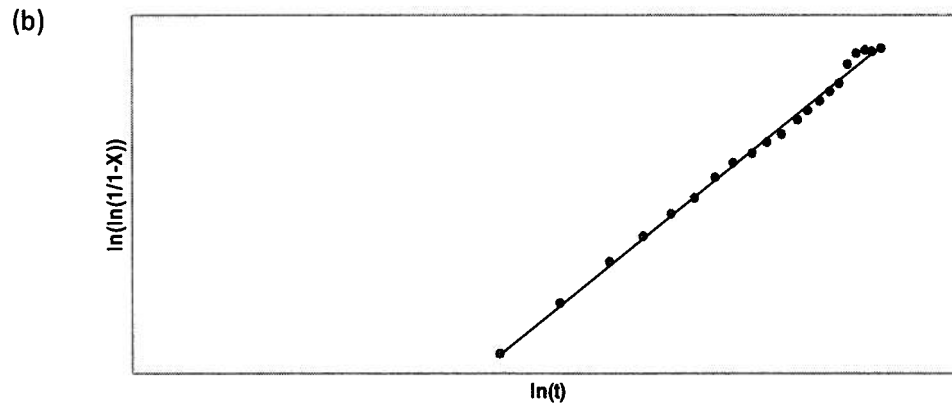
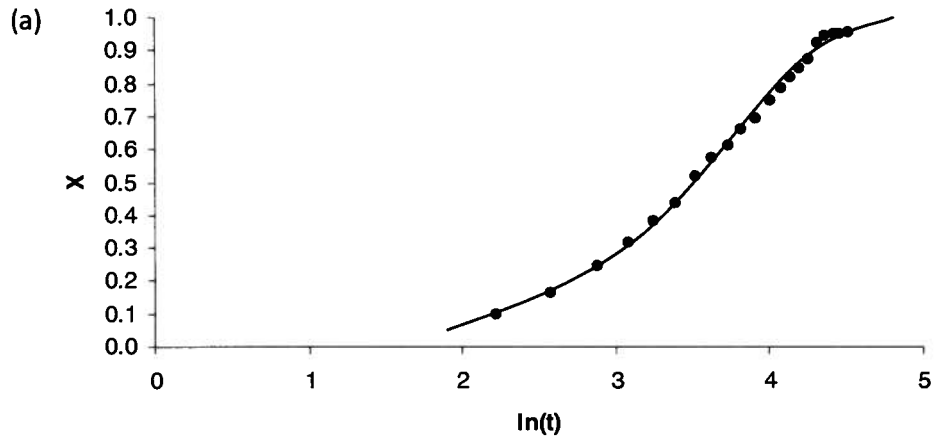


Figure 2. (a) sigmoidal X (fraction DRX) vs. $\ln(t)$ plot (b) straight line plot $\ln(\ln(1/1-X))$ vs. $\ln(t)$.